

ARTICLE

Density functional theory and time-dependent density functional theory studies on optoelectronic properties of fused heterocycles with cyclooctatetraene

Vipin Kumar¹ | Anuj Tripathi¹ | Seyong Choi²  | Ramesh Kumar Chitumalla²  |
Ji-Youn Seo² | Joonkyung Jang²  | Prabhakar Chetti¹ 

¹Department of Chemistry, National Institute of Technology, Kurukshetra, Haryana, India

²Department of Nanoenergy Engineering, Pusan National University, Busan, Republic of Korea

Correspondence

Prabhakar Chetti, Department of Chemistry, National Institute of Technology, Kurukshetra 136119, Haryana, India.

Email: chetty_prabhakar@yahoo.com

Joonkyung Jang, Department of Nanoenergy, Engineering Pusan National University, Busan 46241, Republic of Korea.

Email: jkjang@pusan.ac.kr

Funding information

SERB, Grant/Award Number: SB/FT/CS-101/2014; 2021 BK21 FOUR Program of Pusan National University

Abstract

We establish a structure–property relation for the system having a cyclooctatetraene (COT) ring fused with four five-membered heterocyclic rings. The two five-membered heterocycles selected are furan and selenophene and their fused structure with COT is known as cyclooctatetrafuran (COF) and cyclooctatetraselenophene (COSe), respectively. We found 15 geometrical isomers of each COF and COSe and their structural stability and optoelectronic properties have been evaluated by quantum chemical simulations. The density functional theory (DFT) and time-dependent DFT simulations were employed for a systematic review of all isomers. Electronic excitations, hole reorganization energies, electron reorganization energies, ionization potentials, and electron affinities, of all the isomers, were reported. Based on our comparative study, it is shown that one of the isomers is suggested as a better charge transport material.

KEYWORDS

charge transport, cyclooctatetraene, cyclooctatetrafuran, cyclooctatetraselenophene, optoelectronics

INTRODUCTION

With the continuously growing demand for molecules having remarkable functions, the π -conjugated skeleton due to its dynamic molecular motion has been studied widely. The well-reported molecules showing a dynamic π -system are corannulene and sumanene having a bowl-to-bowl inversion behavior.^{1–3} In continuation to this corannulene and sumanene, cyclooctatetraene (COT) having flexible π -conjugated frameworks is studied both experimentally and theoretically. The D_{2d} symmetry with nonplanar saddle-shaped or tub-shaped geometry results in angle strain and antiaromaticity in COT.^{4–7} However, its planar form is obtained by oxidation and reduction reaction which follow the Huckle rule of aromaticity. These COT-based materials are showing fascinating behavior in design and synthesis as cavity size control cage molecules, buckycatchers, molecular tweezers, and electromechanical actuators.^{8–10}

Tetraphenylene is a widely studied and well-reported molecule that has four benzene rings fused with COT. Due

to the saddle-shaped geometry of tetraphenylene and its derivatives, they find applications in helical framework, molecule clathrates, and catalysts.^{9,11–15} Yamaguchi et al. reported the thiazole fused with COT and showed that the tub-shaped backbone is changing to planar via reduction and oxidation.¹⁶ There are reports in the literature on cyclooctatetraphiophene (COT_h) where thiophene fused with the COT framework.¹⁷ It is also reported that with the presence of electron-rich thiophene on the boundary and having flexible π -conjugated skeletons, COT_h has prominent applications in optoelectronics.^{14,17–19} Considering the connectivity of thiophene, COT_h has 15 isomers, and four of them were synthesized and reported by Wang et al.¹⁷ The different connectivity of thiophene in synthesized isomers of COT_h is confirmed by single-crystal analysis.^{20–22} In our previous work related to thiophene-based organic materials, we have performed a computational study on benzothiophene (BTT) isomers and its oligomer.^{23,24} The theoretical study on the seven possible isomers reveals that the isomers of BTT are better candidates

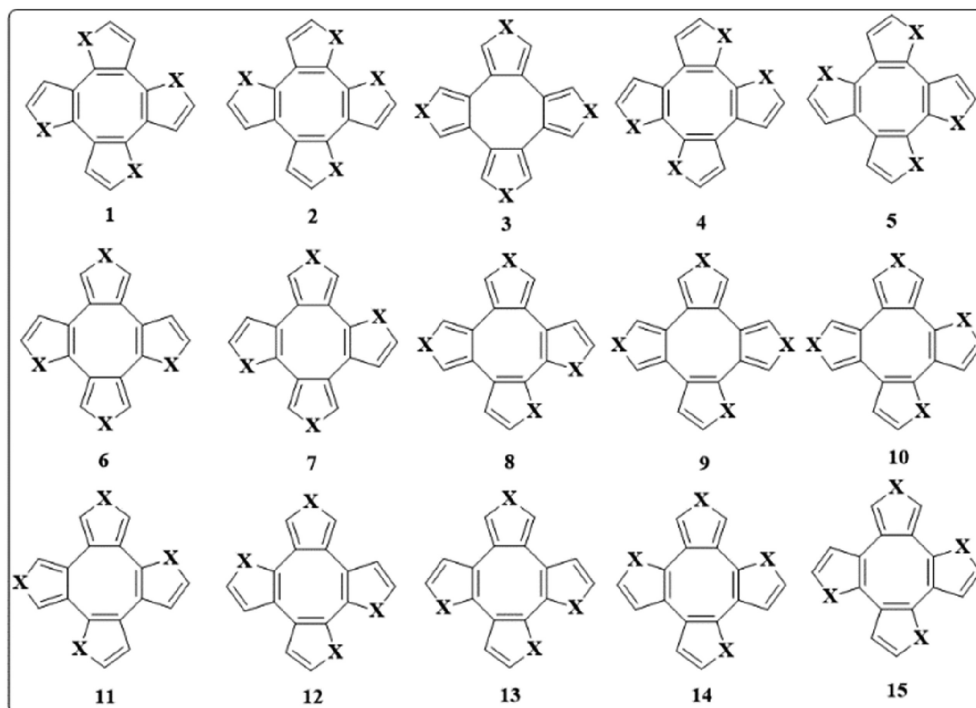


FIGURE 1 Molecular structures of 15 possible isomers of COF (X is O), COTh (X is S), and COSe (X is Se) molecules

as hole and electron transport materials.^{23,24} Further study is extended for comparative study of BTT isomer with different fused heterocycles such as pyrrole (BTP), furan (BTF), and selenophene (BTSe).²⁵

One of our recent works has shown that the COTh has 15 possible isomers and out of these 15 isomers, only five isomers have a synthesis route.²⁷ The calculated UV–visible absorption obtained from time-dependent density functional theory (TDDFT) simulations are reproducing the experimental absorption of known isomers. The previous study also reveals that out of 15 isomers, one of the COTh isomers is showing better reorganization energies than the standard materials.²⁷ Herein, we investigated and compared the optical and charge transfer properties of all the isomers of cyclooctatetrafuran (COF) and cyclooctatetraselenophene (COSe) with those of cyclooctatetrathiophene isomers (COTh).

COMPUTATIONAL METHODS

All the isomers of COF and COSe (Figure 1) are fully optimized using Gaussian 16 software with B3LYP functional in conjunction with the 6-311+G(d,p) basis set.²⁷ The frequency analysis confirmed that the energy-minimized structures have no imaginary frequency. The UV–visible absorption spectra are simulated using TDDFT formalism with B3LYP functional at the same level of theory as used in the optimization.

According to the Marcus Hopping's model, the electron/hole transport process is an electron/hole transfer

reaction between the neighboring molecules²⁹ and the hole transfer can be defined as,



where Q^+ is the cationic state and Q is the neutral state of the molecule. The Marcus equation of rate constant (K) for the charge transfer process is,

$$K = \left(\frac{4\pi^2}{h} \right) \Delta H^2 (4\pi\lambda k_b T)^{-1/2} \exp(-\lambda/4k_b T) \quad (2)$$

where h is the Planck's constant, ΔH is the transfer integral, λ is the reorganization energy, k_b is the Boltzmann constant, and T is the absolute temperature. From Equation (2), it is clear that the K depends on λ and it is inversely proportional to λ .²⁹ The hole and electron reorganization energies (λ_h and λ_e) can be calculated from Equations (3a) and (3b),^{23–26,30} and the detailed procedure is given in the supporting information S1.

$$\lambda_h = \delta_1 + \delta_2 = [E^+(M_0) - E^+(M_+)] + [E^0(M_+) - E^0(M_0)] \quad (3a)$$

$$\lambda_e = \delta_3 + \delta_4 = [E^-(M_0) - E^-(M_-)] + [E^0(M_-) - E^0(M_0)] \quad (3b)$$

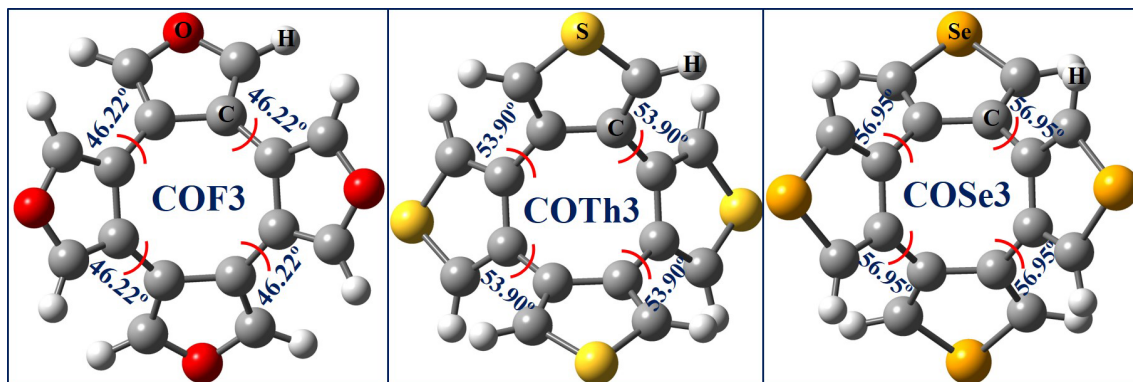


FIGURE 2 Optimized structures and important dihedral angles of the most stable isomer of COF, COTH, and COSe

Also, we have calculated adiabatic and vertical ionization potentials (IP_a and IP_v), and adiabatic and vertical electron affinities (EA_a and EA_v) as in our previous works.^{24–27,31}

RESULTS AND DISCUSSION

Geometry and structures

The optimized geometries of the COF and COSe isomers along with dihedral angles and corresponding relative energies are shown in the Table S1.

Based on the relative energies from Table S1, Isomer 3 of each series is the most stable isomer and the difference between the relative energies of isomers is minimal, that is, less than 10 kcal/mol. The optimized geometries of the most stable isomer in each series are shown in Figure 2.

Among the COF series, the isomer COF3 is found to be more stable than the other isomers by 0.5–10 kcal/mol. It is found that the isomer with a greater number of exocyclic double bonds is more stable than that of a smaller number of exocyclic double bonds. The most stable isomer (COF3) and the second most stable isomers (COF9 and COF6) have eight and six exocyclic double bonds, respectively. The relative energies of COF9 and COF6 are 1.73 and 3.88 kcal/mol, respectively. Similarly, the COF isomers without any exocyclic double bonds (COF1, COF2, COF4, and COF5) have relative energies of more than 5 kcal/mol. Also, a similar trend in the stability of the COSe isomers has been observed. However, in the case of the COSe series, the difference in the energy between the most and least stable isomers is smaller than 5 kcal/mol and this small energy difference can be attributed to the large size of the selenium. Interestingly, the COF and COSe isomers followed the same stability order of $3 > 9 > 6 > 7 > 8 > 10 > 11 > 13 > 12 > 14 > 15 > 4 > 2 > 5 > 1$ which is also the order of decreasing numbers of exocyclic double bonds. The relative energies of COTH, COF, and COSe isomers are plotted and shown in Figure 3.

The dihedral angles observed in COF3 and COSe3 are 46.22° and 56.95° are also the highest dihedral angle in their respective series. As shown in Figure 2, the dihedral

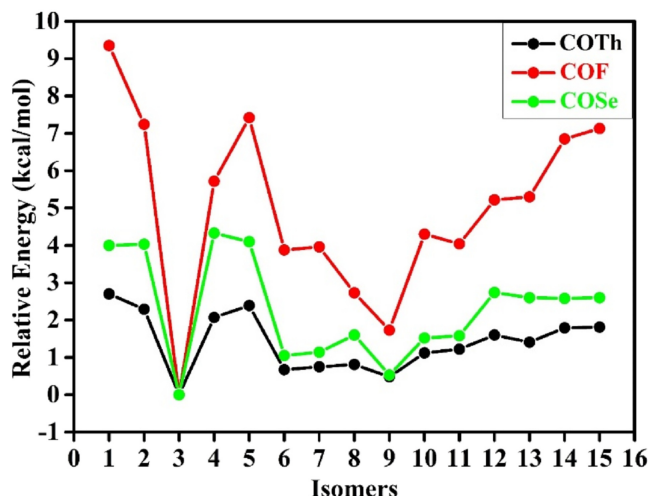


FIGURE 3 Relative energies of the 15 isomers of COTH, COF, and COSe. The energy of Isomer 3 in each series is considered 0.0 kcal/mol.

angle increased with a rise in the heteroatom size ($O \rightarrow S \rightarrow Se$). Interestingly, similar is the case for other isomers, where an increase in the size of heteroatom increased dihedral angle. The optimized geometries of all the isomers of COF, COTH, and COSe with their relative energies and dihedral angles are given in Table S1.

Electronic excitations

As we have already shown in our previous studies of COTH isomers, five isomers are experimentally reported with their absorption properties and our theoretical results reproduced the experimental absorption. Herein, we evaluate the UV-visible absorption properties of COF and COSe isomers with the same methodology. The first three electronic excitations of all the isomers of COF and COSe are summarized in Tables 1 and 2 along with the other optical data, whereas similar data of COTH isomers are shown in Table S2. The optical properties, especially, the vertical excitation energies are more susceptible to the computational method employed. Therefore, it is

TABLE 1 Computed lowest electronic excitations (λ_{cal}), oscillator strength (f), major transition (MT), and % weight of C_i of COF isomers obtained at TD-B3LYP/6-311+G(d,p) level

Isomer	Excitation state	λ_{cal} (nm)	f	MT	% C_i
COF1	S1	292	0.026	H \rightarrow L	99
	S2	272	0.001	H \rightarrow L + 3	56
	S3	262	0.001	H \rightarrow L + 4	96
COF2	S1	440	0.036	H \rightarrow L	99
	S2	293	0.030	H-1 \rightarrow L	72
	S3	263	0.104	H-2 \rightarrow L	65
COF3	S1	247	0.001	H-2 \rightarrow L	88
	S2	241	0.001	H-2 \rightarrow L + 1	49
	S3	232	0.021	H-2 \rightarrow L + 1	36
COF4	S1	418	0.011	H \rightarrow L	99
	S2	307	0.027	H-1 \rightarrow L	66
	S3	270	0.648	H \rightarrow L + 1	66
COF5	S1	436	0.021	H \rightarrow L	99
	S2	302	0.034	H-1 \rightarrow L	68
	S3	281	0.025	H-2 \rightarrow L + 1	65
COF6	S1	307	0.040	H \rightarrow L	98
	S2	299	0.015	H-1 \rightarrow L	60
	S3	276	0.010	H-1 \rightarrow L + 1	97
COF7	S1	306	0.007	H-1 \rightarrow L	97
	S2	297	0.020	H \rightarrow L	64
	S3	273	0.005	H \rightarrow L + 1	96
COF8	S1	315	0.257	H \rightarrow L	97
	S2	283	0.001	H \rightarrow L + 1	51
	S3	276	0.028	H \rightarrow L + 1	50
COF9	S1	272	0.049	H \rightarrow L	48
	S2	268	0.173	H \rightarrow L + 1	47
	S3	259	0.010	H-1 \rightarrow L	37
COF10	S1	315	0.153	H \rightarrow L	94
	S2	276	0.028	H-1 \rightarrow L	75
	S3	273	0.020	H \rightarrow L + 2	48
COF11	S1	310	0.049	H \rightarrow L	92
	S2	286	0.026	H \rightarrow L + 1	90
	S3	271	0.043	H-2 \rightarrow L	87
COF12	S1	363	0.049	H \rightarrow L	97
	S2	309	0.010	H-1 \rightarrow L	55
	S3	278	0.331	H \rightarrow L + 1	50
COF13	S1	371	0.119	H \rightarrow L	97
	S2	305	0.023	H-1 \rightarrow L	64
	S3	276	0.194	H \rightarrow L + 1	53
COF14	S1	371	0.010	H \rightarrow L	98
	S2	317	0.010	H \rightarrow L + 1	56
	S3	278	0.345	H-1 \rightarrow L	50
COF15	S1	375	0.042	H \rightarrow L	98
	S2	312	0.007	H-1 \rightarrow L	51
	S3	277	0.306	H \rightarrow L + 1	46

TABLE 2 Computed lowest electronic excitations (λ_{cal}), oscillator strength (f), major transition (MT), and % weight of C_i of COSe isomers obtained at TD-B3LYP/6-311+G(d,p) level

Isomer	Excitation state	λ_{cal} (nm)	f	MT	% C_i
COSe1	S1	382	0.064	H-1 \rightarrow L	86
	S2	320	0.026	H-3 \rightarrow L	87
	S3	297	0.038	H-2 \rightarrow L	65
COSe2	S1	387	0.022	H \rightarrow L	98
	S2	328	0.014	H-1 \rightarrow L	59
	S3	321	0.067	H-2 \rightarrow L	86
COSe3	S1	277	0.068	H \rightarrow L	94
	S2	273	0.034	H-1 \rightarrow L	91
	S3	265	0.060	H-2 \rightarrow L + 2	31
COSe4	S1	384	0.010	H \rightarrow L	99
	S2	328	0.010	H-1 \rightarrow L	69
	S3	318	0.039	H-2 \rightarrow L	65
COSe5	S1	385	0.014	H \rightarrow L	99
	S2	326	0.020	H-1 \rightarrow L	65
	S3	320	0.062	H-2 \rightarrow L	69
COSe6	S1	312	0.048	H \rightarrow L	86
	S2	307	0.005	H-1 \rightarrow L	62
	S3	306	0.006	H \rightarrow L + 1	68
COSe7	S1	308	0.028	H \rightarrow L	69
	S2	303	0.020	H-1 \rightarrow L + 2	83
	S3	299	0.010	H-1 \rightarrow L + 1	55
COSe8	S1	329	0.118	H \rightarrow L	95
	S2	304	0.018	H-1 \rightarrow L	96
	S3	298	0.088	H-2 \rightarrow L	81
COSe9	S1	300	0.065	H \rightarrow L	75
	S2	292	0.066	H \rightarrow L + 1	72
	S3	287	0.004	H \rightarrow L + 1	88
COSe10	S1	320	0.086	H \rightarrow L	95
	S2	308	0.007	H \rightarrow L + 1	86
	S3	295	0.020	H-2 \rightarrow L	85
COSe11	S1	314	0.058	H \rightarrow L	97
	S2	304	0.017	H \rightarrow L + 1	90
	S3	289	0.002	H \rightarrow L + 2	93
COSe12	S1	345	0.040	H \rightarrow L	96
	S2	327	0.011	H \rightarrow L + 1	79
	S3	311	0.086	H-1 \rightarrow L	73
COSe13	S1	354	0.065	H \rightarrow L	97
	S2	332	0.002	H \rightarrow L + 1	64
	S3	315	0.117	H-1 \rightarrow L	60
COSe14	S1	334	0.019	H \rightarrow L	86
	S2	328	0.024	H \rightarrow L + 1	85
	S3	303	0.040	H-1 \rightarrow L	85
COSe15	S1	342	0.028	H \rightarrow L	97
	S2	326	0.012	H \rightarrow L + 1	80
	S3	307	0.129	H-1 \rightarrow L	74

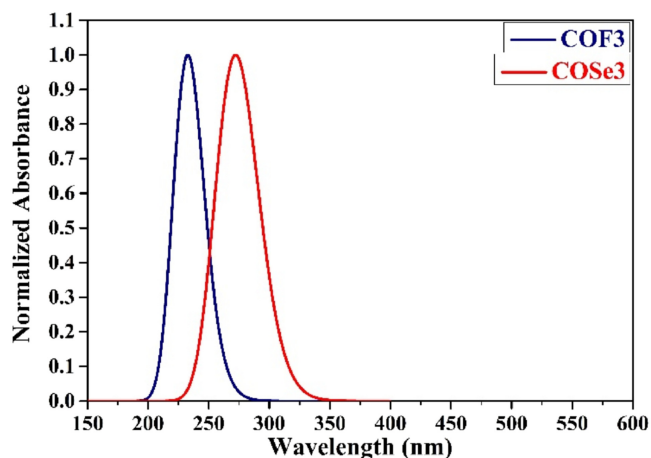


FIGURE 4 Simulated UV-visible absorption spectra of COF3 and COSe3

important to employ various types of density functionals to predict the optical properties.^{31,32} Further, to validate our methodology, different functionals were used in the evaluation of the absorption properties to choose the best among fitted functional for absorption. The UV-visible absorption was simulated with different density functionals, which include hybrid GGA (BH and HLYP, B3LYP, and PBE0), meta-hybrid GGA (M06), and long-range corrected hybrid (CAM-B3LYP and ω B97XD) functionals at a 6-311+G(d,p) basis set to investigate the effect of functionals on the electronic excitations. To the best of our knowledge, Humayun Kabir and Miura synthesized the COF3 isomer³³ and no other isomer of COF is synthesized yet. Asit and Wijsboom synthesized the COSe3 and also reported UV-visible absorption data.³⁴ Only one isomer in each series of COF and COSe was reported experimentally, whereas five isomers (Isomers 1, 2, 4, and 5) in the COTH

TABLE 3 Calculated HOMO, LUMO energies and energy gap (HLG), ionization potentials (IP), electron affinities (EA), and reorganization energies (λ_h and λ_e) at B3LYP/6-311+G(d,p) level of theory

Isomer	HOMO (eV)	LUMO (eV)	HLG (eV)	IPa (eV)	IPv (eV)	EAA (eV)	EAv (eV)	λ_h (meV)	λ_e (meV)
COF isomers									
COF1	-5.28	-1.73	3.55	6.47	6.79	0.66	0.25	560	698
COF2	-5.34	-1.74	3.60	6.51	6.84	0.63	0.26	584	680
COF3	-6.33	-0.72	5.61	7.74	7.83	-0.47	-0.62	197	298
COF4	-5.41	-1.67	3.74	6.59	6.92	0.57	0.19	609	706
COF5	-5.34	-1.71	3.63	6.53	6.85	0.62	0.24	588	700
COF6	-5.87	-1.09	4.78	7.20	7.35	-0.10	-0.36	322	486
COF7	-5.87	-1.09	4.78	7.20	7.35	-0.09	-0.36	319	498
COF8	-5.70	-1.26	4.44	6.96	7.22	0.08	-0.22	469	553
COF9	-5.90	-0.90	5.00	7.26	7.48	-0.31	-0.56	447	553
COF10	-5.67	-1.21	4.46	6.96	7.19	0.06	-0.25	429	578
COF11	-5.70	-1.15	4.55	7.00	7.23	0.02	-0.20	430	518
COF12	-5.55	-1.45	4.10	6.81	7.07	0.31	-0.02	476	594
COF13	-5.16	-1.53	3.63	6.76	7.02	0.36	0.07	470	534
COF14	-5.51	-1.43	4.08	6.80	7.03	0.31	-0.04	427	625
COF15	-5.51	-1.49	4.02	6.75	6.99	0.34	0.02	436	580
COSe isomers									
COSe1	-5.83	-1.86	3.97	6.90	7.16	0.83	0.57	480	503
COSe2	-5.81	-1.89	3.92	6.89	7.14	0.87	0.58	471	556
COSe3	-6.22	-1.81	4.41	7.44	7.54	0.06	-0.06	185	233
COSe4	-5.81	-1.85	3.96	6.89	7.14	0.84	0.56	464	536
COSe5	-5.82	-1.87	3.95	6.89	7.14	0.85	0.57	472	540
COSe6	-5.99	-1.43	4.56	7.19	7.38	0.30	0.15	339	307
COSe7	-6.03	-1.37	4.66	7.19	7.35	0.25	0.08	309	344
COSe8	-5.94	-1.60	4.34	7.04	7.28	0.54	0.29	451	508
COSe9	-6.05	-1.33	4.72	7.20	7.44	0.22	0.03	436	429
COSe10	-5.96	-1.48	4.48	7.07	7.30	0.44	0.22	433	461
COSe11	-5.93	-1.42	4.51	7.09	7.31	0.36	0.16	405	412
COSe12	-5.89	-1.64	4.25	7.00	7.22	0.60	0.34	420	502
COSe13	-5.88	-1.74	4.14	6.97	7.21	0.71	0.44	438	524
COSe14	-5.91	-1.52	4.39	7.03	7.24	0.48	0.22	405	524
COSe15	-5.90	-1.62	4.28	7.00	7.23	0.57	0.34	426	462

series have been synthesized and experimentally reported.²⁶ We compared the experimental UV–visible absorption of five COTH isomers with the TDDFT absorption maxima and the results are in great agreement. As shown in Table S3, the B3LYP functional is reproducing the experimental absorption for five COTH isomers with good accuracy²⁶; hence, further discussion for COF and COSe isomers is based on only B3LYP functional.

As shown in Tables 1 and 2, the first three excitations of COF and COSe isomers are in the range of 250–450 nm. As COTH isomers are discussed in our previous work, here we mainly focus on COF and COSe isomers. Among all isomers of COF and COSe, Isomer 3, the most stable isomers (COF3 and COSe3) are showing the lowest absorption value of 241 and 271 nm, respectively. Isomer 2, COF2 is showing the highest absorption of 440 nm and it arises due to HOMO → LUMO transition. Similar is the case for the COSe2 isomer, it is showing the highest absorption of 387 nm in the COSe series. In comparison with the COTH isomers, it is observed that the replacement of sulfur either with oxygen or with selenium results in a bathochromic shift. For instance, the calculated absorption of COTH7 is showing a 10–12 nm hypsochromic shift as compared to those of COF7 and COSe7. The simulated UV–visible absorption spectra of COF3 and COSe3 are depicted in Figure 4, whereas the UV–visible absorption spectra of the COF, COSe, and, COTH isomers are shown in Figure S1.

Frontier molecular orbitals

The eigenvalues of the frontier molecular orbitals and HOMO–LUMO gap (HLG) are summarized in Table 3. The highest HLG is observed for Isomer 3 of each series and their HLGs are 5.61 eV and 4.41 eV for COF3 and COSe3,

respectively. In Figure 5, the comparison of the energy gap of the most stable isomers in each series is shown with their molecular orbitals. Interestingly, the HOMO levels of COF3 and COSe3 are close with HOMO energies of −6.33 and −6.22 eV, respectively. However, furan as heterocycle results in destabilization of LUMO level, which in turn increases the HLG of COF3 by 0.29 eV. On the other hand, with selenophene heterocycle results in stabilization of LUMO resulting in a significant lowering in HLG of COSe3 by 0.91 eV.

The calculated HLG of COF1 and COSe1 are 3.63 and 3.92 eV, respectively, and are the smallest among isomers of respective series. Figure 6 depicts the electron density distribution and comparison of the HLGs for the COF and COSe isomers with the smallest, largest, and intermediate

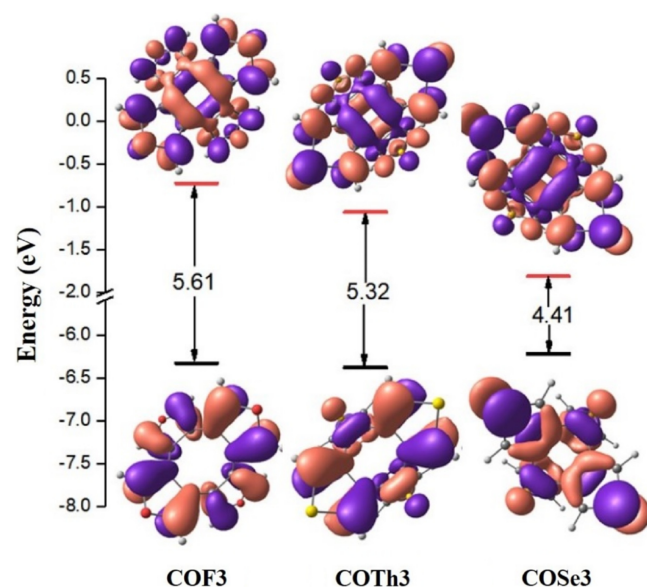


FIGURE 5 Isodensity surfaces of frontier molecular orbitals with the corresponding energy gap of the most stable isomer of each series

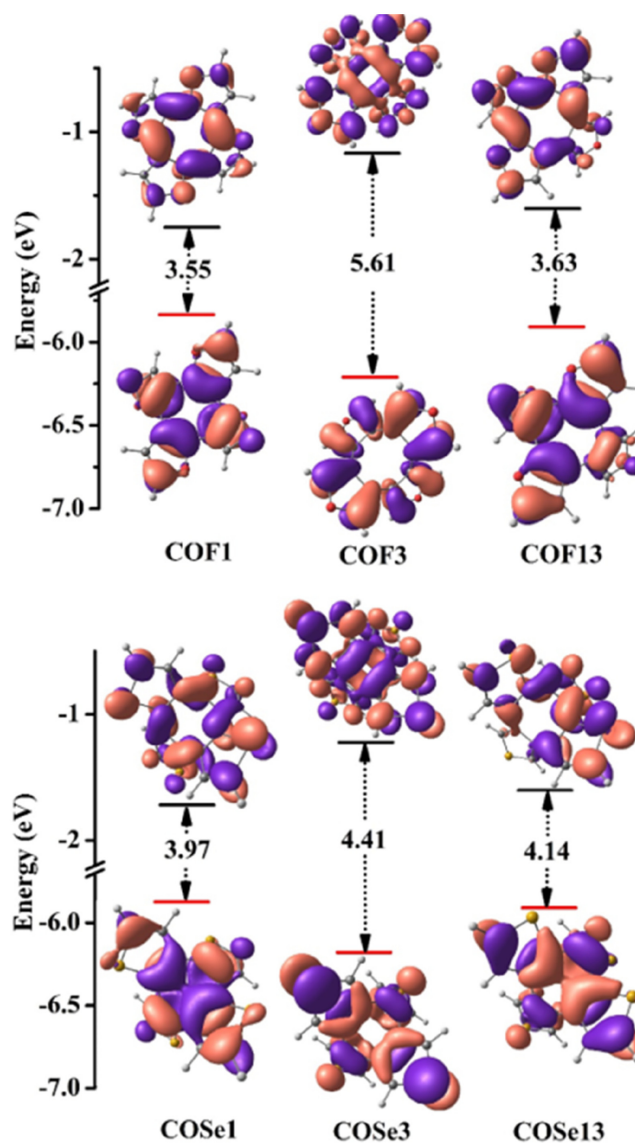


FIGURE 6 Isodensity surfaces of frontier molecular orbitals with the corresponding energy gap of isomers 1, 3, and 13 of COF (top) COSe (bottom)

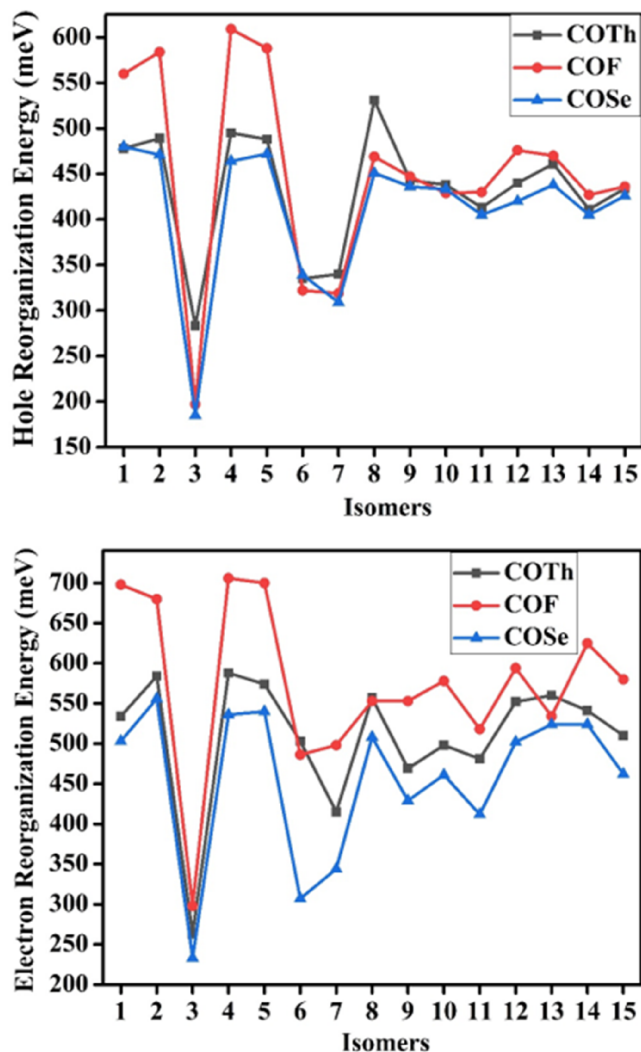


FIGURE 7 Calculated hole (top) and electron (bottom) reorganization energies of COT, COF, and COSe isomers

HLGs, whereas a similar comparison of the three COT isomers is shown in Figure S2.

Ionization potential, electron affinity, and reorganization energy

The ionization potential (IP) and electron affinity (EA) are two important factors in the charge injection phenomenon. A low IP and high EA favor the performance of an optoelectronic device. The calculated IPs and EAs of COF and COSe isomers are shown in Table 3 (COT data in Table S4). The Isomers 1, 2, 4, and 5 of each series have shown small adiabatic and vertical IPs. However, furan fused COT isomers are showing smaller IPs as compared to those of thiophene and selenophene fused COT isomers. The smaller IPs of the COF isomers indicate that it is easy to create a hole in the COF isomer as compared to the corresponding COT and COSe

isomer. On the other hand, the EA of the COSe isomer is higher than the corresponding COF or COT isomer suggesting it is easy to inject electrons into the COSe isomer.

It is evident from Equation (2), the smaller reorganization energy leads to a higher rate constant which favors the charge transport. The simulated hole (λ_h) and electron (λ_e) reorganization energies of COF and COSe isomers are summarized in Table 3 (COT data in Table S4). It can be observed from Table 3 that the isomers showed high reorganization energies (λ_h and λ_e) ranging from 200 to 600 meV. The third isomer of each series showed the smallest hole reorganization energy and electron reorganization energy in their respective series. The hole and electron reorganization energies of COT, COF, and COSe isomers were plotted and shown in Figure 7. The calculated hole reorganization energies of COT3, COF3, and COSe3 are 283, 197, and 185 meV, respectively, and are smaller than that of the TPD molecule,³⁶ a typical hole transport material with a hole reorganization energy of 290 meV. Similarly, the calculated electron reorganization energy for COT3, COF3, and COSe3 are 263, 298, and 233 meV, respectively, and are comparable to or smaller than that of Alq3,³⁷ a typical electron transport material with an electron reorganization energy of 276 meV.

CONCLUSION

A detailed comparative theoretical investigation on possible isomers of COF, COT, and COSe has been carried out employing DFT and TDDFT simulations. Among 15 isomers, Isomer 3 of each series is the most stable isomer and this stability is attributed to the maximum number of exocyclic double bonds. The simulated UV-visible absorption spectra are in excellent agreement with the absorption range of experimentally reported isomers. Within each series, the second and third isomers are showing the highest and the lowest absorption, respectively. The replacement of thiophene with furan (selenophene) shows destabilization (stabilization) of LUMO, which increased (decreased) HLG. Smaller hole and electron reorganization energies of the third isomer of each series than that of standard materials show that the studied isomers are better hole and electron transport materials. The investigated isomers in this study may expand the COT family for both organic synthesis and organic electronics.


ACKNOWLEDGMENTS

This research was supported by SERB, New Delhi, India (SB/FT/CS-101/2014) and 2021 BK21 FOUR Program of Pusan National University.

CONFLICT OF INTEREST

The authors declare no conflict of interest.

ORCID

Seyong Choi  <https://orcid.org/0000-0002-4888-5376>Ramesh Kumar Chitumalla  <https://orcid.org/0000-0002-9523-7056>Joonkyung Jang  <https://orcid.org/0000-0001-9028-0605>Prabhakar Chetti  <https://orcid.org/0000-0003-1773-9429>

REFERENCES

- [1] T. J. Seiders, K. K. Baldrige, G. H. Grube, J. S. Siegel, *J. Am. Chem. Soc.* **2001**, 123, 517.
- [2] A. Sygula, *Eur. J. Org. Chem.* **2011**, 2011, 1611.
- [3] T. Amaya, H. Sakane, T. Muneishi, T. Hirao, *Chem. Commun.* **2008**, 8, 765.
- [4] T. Nishinaga, T. Uto, R. Inoue, A. Matsuura, N. Treitel, M. Rabinovitz, K. Komatsu, *Chem. – Eur. J.* **2008**, 14, 2067.
- [5] C. S. Wannere, D. Moran, N. L. Allinger, B. A. Hess, L. J. Schaad, P. V. R. Schleyer, *Org. Lett.* **2003**, 5, 2983.
- [6] C. Trindle, *J. Org. Chem.* **1991**, 56, 5427.
- [7] D. S. Kumml, S. Lobsiger, H. M. Frey, S. Leutwyler, J. F. Stanton, *J. Phys. Chem. A* **2008**, 112, 9134.
- [8] A. Sygula, F. R. Fronczek, R. Sygula, P. W. Rabideau, M. M. Olmstead, *J. Am. Chem. Soc.* **2007**, 129, 3842.
- [9] T. Nishiuchi, Y. Kuwatani, T. Nishinaga, M. Iyoda, *Chem. – Eur. J.* **2009**, 15, 6838.
- [10] H.-Y. Peng, C.-K. Lam, T. C. W. Mak, Z. Cai, W.-T. Ma, Y.-X. Li, H. N. C. Wong, *J. Am. Chem. Soc.* **2005**, 127, 9603.
- [11] T. Nishinaga, T. Ohmae, K. Aita, M. Takase, M. Iyoda, T. Arai, Y. Kunugi, *Chem. Commun.* **2013**, 49, 5354.
- [12] W. S. Rapson, R. G. Shuttleworth, J. N. van Niekerk, *J. Chem. Soc.* **1943**, 326.
- [13] H. N. C. Wong, *Acc. Chem. Res.* **1989**, 22, 145.
- [14] H. Huang, T. Stewart, M. Gutmann, T. Ohhara, N. Niimura, Y.-X. Li, J.-F. Wen, R. Bau, H. N. C. Wong, *J. Org. Chem.* **2009**, 74, 359.
- [15] M. J. Marsella, I. T. Kim, F. Tharn, *J. Am. Chem. Soc.* **2000**, 122, 974.
- [16] Y.-M. Man, T. C. W. Mak, H. N. C. Wong, *J. Org. Chem.* **1990**, 55, 3214.
- [17] K. Mouri, S. Saito, S. Yamaguchi, *Angew. Chem., Int. Ed.* **2012**, 124, 6173.
- [18] C. Zhao, L. Xu, Y. Wang, C. Li, H. Wang, *Chin. J. Chem.* **2014**, 33, 71.
- [19] B. Greving, A. Woltermann, T. Kauffmann, *Angew. Chem., Int. Ed.* **1974**, 13, 467.
- [20] M. J. Marsella, R. J. Reid, S. Estassi, L.-S. Wang, *J. Am. Chem. Soc.* **2002**, 124, 12507.
- [21] Y. Wang, J. Song, L. Xu, Y. Kan, J. Shi, H. Wang, *J. Org. Chem.* **2014**, 79, 2255.
- [22] Y. Wang, Z. Wang, D. Zhao, Z. Wang, Y. Cheng, H. Wang, *Synlett* **2007**, 15, 2390.
- [23] Y. Wang, D. Ga, J. Shi, Y. Kan, J. Song, C. Li, H. Wang, *Tetrahedron* **2014**, 70, 631.
- [24] A. Tripathi, C. Prabhakar, *J. Chin. Chem. Soc.* **2019**, 66(8), 891.
- [25] A. Tripathi, O. Kozaderov, K. Shikhaliev, C. Prabhakar, *J. Phys. Org. Chem.* **2020**, 33(3), e4037.
- [26] A. Tripathi, C. Prabhakar, *Mol. Sim.* **2020**, 46, 548.
- [27] A. Tripathi, V. Kumar, C. Prabhakar, *J. Sulfur Chem.* **2022**, 43, 180.
- [28] M. J. Frisch, G. W. Trucks, H. B. Schlegel, G. E. Scuseria, M. A. Robb, J. R. Cheeseman, G. Scalmani, V. Barone, B. Mennucci, G. A. Petersson, H. Nakatsuji, M. Caricato, X. Li, H. P. Hratchian, A. F. Izmaylov, J. Bloino, G. Zheng, J. L. Sonnenberg, M. Hada, M. Ehara, K. Toyota, R. Fukuda, J. Hasegawa, M. Ishida, T. Nakajima, Y. Honda, O. Kitao, H. Nakai, T. Vreven, M. JA, J. E. Peralta, F. Ogliaro, M. Bearpark, J. J. Heyd, E. Brothers, K. N. Kudin, V. N. Staroverov, R. Kobayashi, J. Normand, K. Raghavachari, A. Rendell, J. C. Burant, S. S. Iyengar, J. Tomasi, M. Cossi, N. Rega, J. M. Millam, M. Klene, J. E. Knox, J. B. Cross, V. Bakken, C. Adamo, J. Jaramillo, R. Gomperts, R. E. Stratmann, O. Yazyev, A. J. Austin, R. Cammi, C. Pomelli, J. W. Ochterski, R. L. Martin, K. Morokuma, V. G. Zakrzewski, G. A. Voth, P. Salvador, J. J. Dannenberg, S. Dapprich, A. D. Daniels, O. Farkas, J. B. Foresman, J. V. Ortiz, J. Cioslowski, D. J. Fox, *Gaussian 16, Revision B.01*, Gaussian, Inc, Wallingford, CT **2016**.
- [29] R. A. Marcus, N. Sutin, *Biophys. Acta* **1985**, 811, 265.
- [30] S. F. Nelsen, D. A. Trieber, R. F. Ismagilov, Y. Teki, *J. Am. Chem. Soc.* **2001**, 123, 5684.
- [31] A. Tripathi, C. Prabhakar, *J. Mol. Struct.* **2020**, 1203, 127397.
- [32] S. U. Lee, *Bull. Korean Chem. Soc.* **2013**, 34, 2276.
- [33] E. Choi, C. H. Lee, B. Jun, E. B. Nam, H. Jeong, S. U. Lee, *Bull. Korean Chem. Soc.* **2018**, 39, 858.
- [34] S. M. Humayun Kabir, M. Miura, *Heterocycles* **2000**, 52, 2.
- [35] P. Asit, Y. H. Wijsboom, *Angew. Chem., Int. Ed.* **2007**, 46, 8814.
- [36] M. Malagoli, J. L. Bredas, *Chem. Phys. Lett.* **2000**, 327, 13.
- [37] B. C. Lin, C. P. Cheng, Z. Q. You, C. P. Hsu, *J. Am. Chem. Soc.* **2005**, 127, 66.

SUPPORTING INFORMATION

Additional supporting information may be found in the online version of the article at the publisher's website.

How to cite this article: V. Kumar, A. Tripathi, S. Choi, R. K. Chitumalla, J.-Y. Seo, J. Jang, P. Chetti, *Bull. Korean Chem. Soc.* **2022**, 43(7), 990. <https://doi.org/10.1002/bkcs.12573>